NANO LETTERS

2006
Vol. 6, No. 4
740−743

Mechanically Tunable Three-Dimensional Elastomeric Network/Air Structures via Interference Lithography

Ji-Hyun Jang,[†] Chaitanya K. Ullal,[†] Taras Gorishnyy,[†] Vladimir V. Tsukruk,[‡] and Edwin L. Thomas*,[†]

Institute for Soldier Nanotechnologies, Department of Materials Science and Engineering, Massachusetts Institute of Technology, Cambridge, Massachusetts 02139, and Department of Materials Science and Engineering, Iowa State University, Ames, Iowa 50011

Received December 30, 2005; Revised Manuscript Received February 24, 2006

ABSTRACT

We show how to employ an interference lithographic template (ILT) as a facile mold for fabricating three-dimensional bicontinuous PDMS (poly(dimethylsiloxane)) elastomeric structures and demonstrate the use of such a structure as a mechanically tunable PDMS/air phononic crystal. A positive photoresist was used to make the ILT, and after infiltration with PDMS, the resist was removed in a water-based basic solution which avoided PDMS swelling or pattern collapse occurring during the ILT removal process. Since the period of the structure is approximately 1 μm, the density of states of gigahertz phonons are altered by the phononic PDMS/air crystal. Brillouin light scattering (BLS) was employed to measure phononic modes of the structure as a function of mechanical strain. The results demonstrate that the phononic band diagram of such structures can be tuned mechanically.

Poly(dimethylsiloxane) (PDMS) has proven to be an outstanding material for micro- and nanotechnology.[1] For example, PDMS has been employed to make two-dimensional (2D) and three-dimensional (3D) microfludic devices such as pumps, valves, channels, and cell culture systems.[2,3] PDMS can be deformed reversibly and repeatedly without residual distortion and is thermally stable, inexpensive, nontoxic, and commercially available. Although PDMS can potentially be cross-linked using light,[4] it is not generally used as a photoresist due to the rather inconvenient processing conditions.[5,6] 2D periodic structures patterned by photolithography and then subsequently replicated in PDMS have been demonstrated as deformable optical and acoustic components such as lenses, waveguides, and couplers.[7,8] The relatively low modulus of PDMS (∼2 MPa) can lead to distortions such as feature−feature pairing and feature sagging in conventional microcontact printing of surface features with high-aspect ratio.[9−11] In structures fabricated by microcontact printing or replica molding, which can possess residual physical stresses from the molding procedure, collapse of structures begins to occur at an aspect ratio of around 2.[1,11]

3D periodic submicrometer structures are emerging as a multifunctional materials platform with promise for applications in MEMS, optics, and acoustics including tunable photonic and phononic crystals. Thus far, 3D PDMS structures have only been made by a layer-by-layer approach. The principal disadvantages of this approach are that it is quite time-consuming and requires registration of subsequent layers.[12] Alternatively, the fabrication of complex 3D microchannels has also been demonstrated, albeit at the scale of hundreds of micrometers.[13] To date, microfabrication of 3D elastomeric structures with complex architectures and submicrometer dimensions has not been accomplished. The topological interconnections of the PDMS and template in a bicontinuous 3D network structure mean that simply peeling away the PDMS from the template as is conveniently done in 2D is not possible. The template must therefore be removed by dissolution. A concern of this approach is the potential swelling of PDMS by nonpolar organic solvents such as hexane and toluene.[14,15] Indeed, we have found that even polar organic solvents (alcohol, acetone, etc.) cause sufficient swelling of the PDMS to prevent their use as developers. Since PDMS is swollen much less by water and is compatible with some inorganic bases,[16] we chose a water-based basic solution (diluted AZ-400K developer) to remove the template.

The use of multibeam interference lithography provides a promising approach to the fabrication of large-area and periodic 3D templates on the submicrometer scale both rapidly and cheaply.[17] Importantly it affords control over

* Corresponding author: tel, 617-253-5931; fax, 617-253-5859; e-mail, elt@mit.edu.
[†] Massachusetts Institute of Technology.
[‡] Iowa State University.

10.1021/nl052577q CCC: $33.50
Published on Web 03/15/2006

geometrical elements of the structures such as symmetry and volume fraction.[18] Interference lithography (IL) involves the transfer of a periodic intensity pattern formed by the interference of multiple beams of light into a photoresist. In a negative photoresist, regions of high light intensity are rendered insoluble via photopolymerization and cross-linking. Most negative resists also undergo shrinkage from photopolymerization and cross-linking, and these materials are prone to swelling in organic developers.[19] Moreover, after PDMS is templated around a negative resist, removal of the cross-linked resist may require rather extreme processing such as resist burning or plasma etching[20,21] and results in damage to the templated material.

Positive photoresists offer an alternative and superior approach for 3D interference lithographic templates (ILTs).[22] In the case of a positive resist, the regions of high light intensity become more soluble. Positive resists have the advantage over negative resists in that they do not undergo shrinkage from polymerization and cross-linking and positive resists can be easily removed in a proper solvent after infiltration. Furthermore, they typically have higher resolution than negative resists since they do not swell in water-based developing solutions after infiltration.[23,24]

Here we report a method for the fabrication of bicontinuous polymer/air 3D elastomeric PDMS using a positive resist ILT. We exploit the elastic nature of these PDMS structures to show that the phononic dispersion relation can be tuned mechanically. This is an important step toward the practical realization of tunable phononic crystals—materials, which forbid propagation of mechanical waves within a certain frequency range (phononic band gap). Structures with submicrometer lattice constants allow control over *hypersonic* waves, valuable for applications in acousto-optics, electron−phonon engineering, and heat management.[25]

Figure 1 shows the three steps of the fabrication process for the 3D elastomeric network/air materials. In the first step, a 3D ILT is fabricated in a positive resist by a single exposure to a periodic light intensity distribution, followed by development (Figure 1a,b). Due to the high surface tension of water, which can potentially cause the pattern to collapse, supercritical drying has been suggested in the case of aqueous-based photoresist.[26] However, supercritical drying of our photoresist resulted in the formation of cracks. Therefore we replaced water with pentane, which has a lower surface tension (73.05 mN/m for water and 13.72 mN/m for pentane at 20 °C[27]).

In the second step, the open 3D network structure is completely filled with PDMS prepolymer via vacuum-assisted infiltration and the PDMS cured in the dark (Figure 1c and Figure 1Sc in Supporting Information). Finally, in step three, a second flood exposure to UV light is done to make the template easily soluble in a dilute basic solution. PDMS is transparent in the UV−vis region and does not prevent the radiation from reaching the template.[1] Upon the second exposure, the diazonaphthoquinone, which still remains in the initially unexposed regions, changes into carboxylic acid and renders the template soluble in basic solution (see Supporting Information).

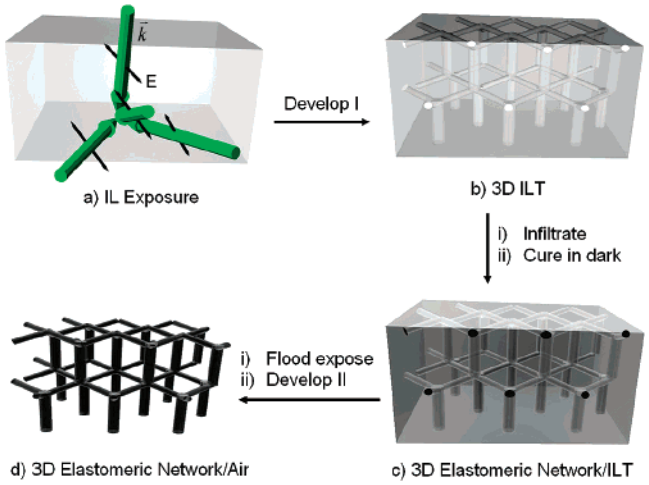

Figure 1. Schematic illustration showing the fabrication process for the 3D continuous elastomeric network/air structure. (a) Exposure by interference lithography (IL). Large arrows show the direction of the beam while small arrows show the direction of polarization of each beam. (b) 3D interference lithography template (ILT) fabricated on positive resist. (c) 3D elastomeric network/ILT structure from the replication of the PDMS onto the ILT. (d) 3D elastomeric network/air structure after flood exposure under UV lamp and subsequent removal of template in a water-based developing solution.

The periodic intensity pattern that will become the void space for templating the PDMS is formed by the interference of four laser beams from the output of a 532 nm continuous wave, frequency-doubled Nd:YVO_4 laser. The Gaussian output from the laser was converted into a top hat function using a refractive beam shaper. The light intensity distribution depends on the relative directions and polarizations of the interfering beams. The overall film thickness is limited by absorption of the photoresist at 532 nm. The attenuation coefficient of AZ-5214-E is $k = 0.0028$ (from ellipsometric measurements), which readily permits pattern thicknesses of 3 μm. The refractive index of AZ5214-E is $n = 1.66$ at 532 nm and is not changed detectably during exposure (measured on a M-2000D ellipsometer from J. A. Woollam Co.). The beam directions and polarizations in air, and hence resultant structure, are the same as those used in ref 28. These are also the same beam directions but different polarizations as those specified in ref 17, resulting in a very similar structure.

The final directions and polarizations of the beams inside the photoresist are given by

$$\vec{k}_0 = [0.0112, 0.0112, 0.0112]\ \vec{E}_0 = [0, -5.74, 5.74]$$
$$\vec{k}_1 = [0.0164, 0.0073, 0.0073]\ \vec{E}_1 = [0, -2.45, 2.45]$$
$$\vec{k}_2 = [0.0073, 0.0164, 0.0073]\ \vec{E}_2 = [0.97, -1.75, 2.97]$$
$$\vec{k}_3 = [0.0073, 0.0073, 0.0164]\ \vec{E}_3 = [-0.97, -2.97, 1.75]$$

where $\vec{k}_i$ and $\vec{E}_i$ are the wave vector and polarizations of the ith beam, respectively. The isosurface of the theoretical light intensity model is shown in Figure 2a. The 3D structure is a four-functional network with symmetry corresponding approximately to the $R\bar{3}m$ space group. The basic motif is

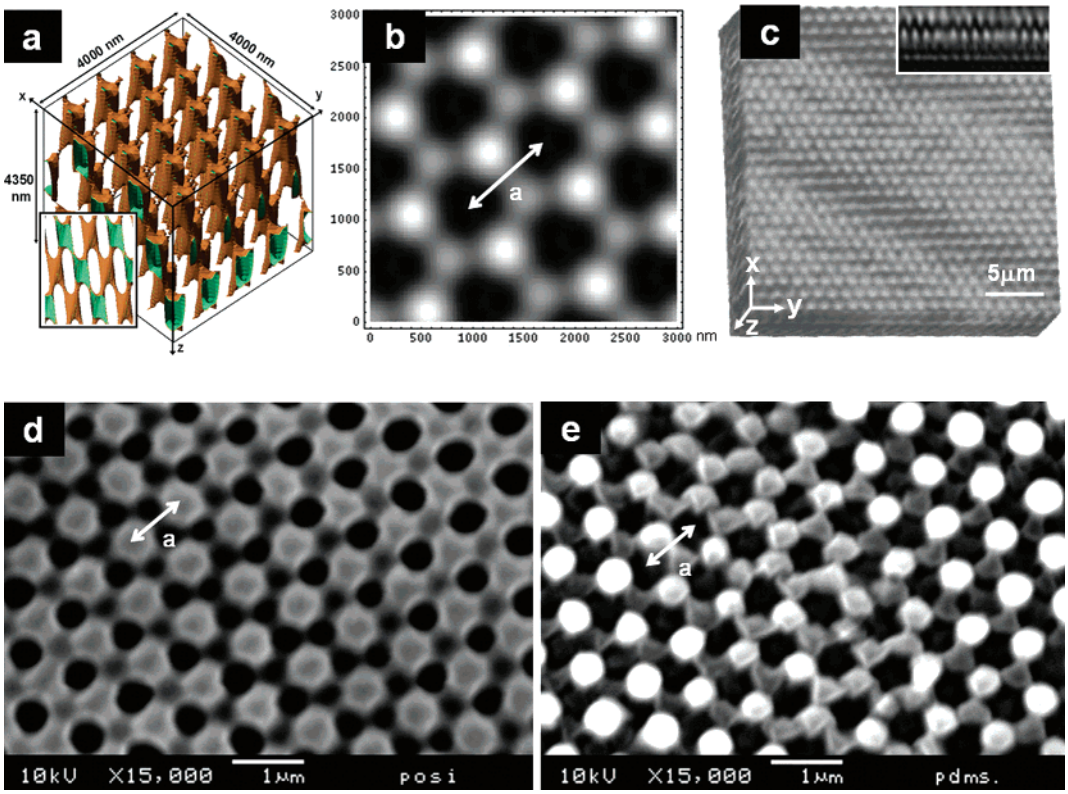

Figure 2. Comparison of theoretical and experimental structures. (a) Isosurface of theoretical light intensity model. The brown and green colors correspond to the inner and outer surfaces, respectively. The inset is view normal to the $(11\bar{2}0)$ planes of the structure. (b) Calculated 3D light intensity profile interference in the (0001) plane. (c) Reconstructed confocal image showing a perspective view of the PDMS elastomeric structure. The inset is the view of $y-z$ cross-sectional plane of the structure corresponding to the schematic views in the inset of (a). (d) SEM image of ILT pattern fabricated in a positive photoresist (AZ5214-E)) with a lattice spacing of 980 nm. (e) SEM image of 3D templated PDMS network/air structure having the complementary structure to (d).

comprised of a vertical post 1100 nm in length and 500 nm in diameter with three shorter struts directed outward from the post, as shown in the inset. Despite aspect ratios of about 2, our structures do not collapse which can be attributed to both the interconnected nature of our structure and a lower residual stress.

Figure 2a shows the isosurface of theoretical light intensity model. The inset is a view normal to the $(11\bar{2}0)$ planes of the structure. Figure 2c is a confocal micrograph and the inset is the $y-z$ cross-section image demonstrating good correspondence with the schematic view shown in the inset of Figure 2a. The PDMS elastomeric structure is the complement of the positive resist template and very closely resembles the light intensity pattern displayed in Figure 2b (compare parts b and e of Figure 2). The expected periodicity ("a" in Figure 2b) in the (0001) plane based on the ILT parameters is 980 nm, and this agrees with the SEM images of the (0001) plane of the experimental structure (Figure 2d,e), confirming that the transfer of the light intensity pattern into PDMS via ILT occurs with high fidelity. The larger scale periodicity in the confocal and SEM images is caused by the photoresist surface being at a slight angle to the (0001) plane of the interference pattern.

In situ monitoring of the PDMS under tensile in-plane deformation was conducted by securing the PDMS sample in a microstretcher mounted on an atomic force microscope stage (AFM). AFM images (Figure 3b,d) show the details

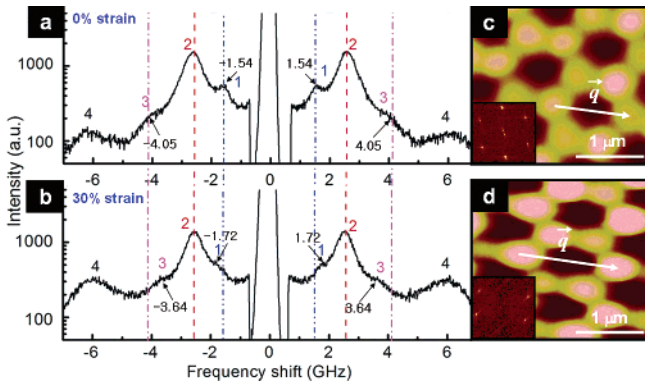

Figure 3. BLS spectra of PDMS elastomeric structures at $|\bar{q}| = 13.88\ \mu m^{-1}$ (72° scattering angle) with 0% (a) and 30% tensile strain (c) along the $[10\bar{1}0]$ direction. Peaks (1) and (3) derive from the phonons propagating in the phononic crystal and are shifted by the deformation. Peak (2) arises from the longitudinal phonons of the unpatterned PDMS substrate and remains unchanged. Peak (4) is a result of backscattered light. The phonon wave vector is oriented along the $[10\bar{1}0]$ direction. AFM images with 0% (b) and 30% tensile strain (d) along the same direction clearly show the change in lattice parameter and symmetry upon deformation. Insets are FFT of the AFM images.

of the change in the sample lattice parameter and symmetry due to the 30% unidirectional strain applied along the $[10\bar{1}0]$ direction. As clear from this image, the unit cell size along the tensile strain direction increases by 30% accompanied

by the reduction of spacing in transverse direction thus demonstrating affine deformation of PDMS structure.

BLS was employed to obtain information about the phononic dispersion relation of the PDMS elastomeric crystals. In Brillouin experiments light is scattered inelastically by thermal phonons. BLS allows for the simultaneous determination of phonon frequency and wave vector by measuring the frequency shift of the scattered light at a known scattering angle. The amplitude of the phonon wave vector can be selected by adjusting the scattering angle, while its orientation with respect to the crystal lattice can be chosen by rotating the sample in the plane perpendicular to the scattering plane (the scattering plane is defined by the incident and the scattered laser beams). Both incident and scattered light are polarized normal to the scattering plane (s-polarized). The frequencies of various phonon modes are obtained by numerical fitting of the experimental data with multiple Lorentzian peaks.

The corresponding BLS spectra exhibit four peaks, see parts a and c of Figure 3 for the spectra of undeformed and deformed sample, respectively. Relatively weak peaks (1) and (3) come from quasi-longitudinal phonons propagating in the PDMS pattern, while a much stronger peak (2) results from the scattering by longitudinal phonons in the unpatterned PDMS substrate. The magnitude of the phonon wave vector for peak (4) is always twice that of the photon wave vector and does not depend on the scattering angle. This q-independent high-frequency peak (4) arises from the contribution of light backscattered by phonons (by 180°) that is then elastically reflected from the front surface of the sample. Note that the position of the substrate peak (2) is unchanged during deformation, while peaks arising from the PDMS/air structure shift from 1.54 to 1.72 GHz and from 4.05 to 3.64 GHz (peaks (1) and (3), respectively). The main source of these peak shifts is the change in size and symmetry of the Brillouin zone. To understand this behavior note that peaks (1) and (3) belong to different phononic bands of the crystal and, as a result, are subject to different crystal momentum conservation laws. In particular, for peak (1) $\vec{q} = \vec{q}_0 - \vec{G}$ and $f = c(|\vec{q}_0 - \vec{G}|)$, while for peak (3) $\vec{q} = \vec{q}_0 + \vec{G}$ and $f = c(|\vec{q}_0 + \vec{G}|)$, where f is the peak frequency, c is the sound velocity, $\vec{q}_0$ is the reduced momentum, and $\vec{G}$ is the reciprocal lattice vector pointing along the $[10\bar{1}0]$ direction. During deformation $\vec{G}$ decreases, which leads to the increase of the frequency of peak (1) and the reduction of the frequency of peak (3).

Experimentally monitoring the modification of the phononic band diagram during the deformation allows the investigation of the influence of symmetry on wave propagation in a crystal. Furthermore, tuning of the dispersion relation in the propagation bands is crucial for the realization of negative refraction materials, superlenses, etc. Moreover, measurement of the directional dependence of sound velocities with BLS can provide important information concerning the elastic constants of transparent crystals and how these change with applied strain.

In summary, 3D elastomeric PDMS/air network structures were successfully fabricated from a positive resist through an ILT. We demonstrated that phononic modes in these elastomeric structures can be tuned mechanically.

Acknowledgment. We specially thank W. Lee, T. Choi, M. Lemieux, J. Walish, and S. Kooi for technical assistance. This work is supported in part by the Postdoctoral Fellowship Program of Korea Science & Engineering Foundation, the Institute for Soldier Nanotechnologies of the U.S. Army Research Office (under Contract DAAD-19-02-0002), the National Science Foundation Grant No. DMR-0414974 and DMR-0308133, and Air Force Office of Scientific Research Grant No. F49620-02-1-0205 and FA9550-05-1-0209.

Supporting Information Available: A description of the chemistry of the positive resist and more detailed experimental procedures. This material is available free of charge via the Internet at http://pubs.acs.org.

References

(1) Xia, Y.; Whitesides, G. M. *Angew. Chem., Int. Ed.* **1998**, *37*, 550.
(2) Chiu, D. T.; Jeon, N. L.; Huang, S.; Kene, R. S.; Wargo, C. J.; Choi, I. S.; Ingber, D. E.; Whitesides, G. M. *Proc. Natl. Acad. Sci. U.S.A.* **2000**, *97*, 2408.
(3) McDonald, J. C.; Whitesides, G. M. *Acc. Chem. Res.* **2002**, *35*, 491.
(4) Choi, K. M.; Rogers, J. A. *J. Am. Chem. Soc.* **2003**, *125*, 4060.
(5) Ryu, K. S.; Wang, X.; Shaikh, K.; Liu, C. *IEEE, J. Microelectromech. Syst.* **2004**, *13*, 568.
(6) Chiang, W.-Y.; Shu, W.-J. *J. Appl. Polym. Sci.* **1988**, *36*, 1889.
(7) Rogers, J. A.; Schueller, O. J. A.; Marzolin, C.; Whitesides, G. M. *Appl. Opt.* **1997**, *36*, 5792.
(8) Wilbur, J. L.; Jackman, R. J.; Whitesides, G. M.; Cheung, E. L.; Lee, L. K.; Prentiss, M. G. *Chem. Mater.* **1996**, *8*, 1380.
(9) Tanaka, T.; Morigami, M.; Atoda, N. *Jpn. J. Appl. Phys.* **1993**, *32*, 6059.
(10) Delamarche, E.; Schmid, H.; Biebuyck, H. A.; Michel, B. *Adv. Mater.* **1997**, *9*, 741.
(11) Lee, T.-W.; Mitrofanov, O.; Hsu, J. W. P. *Adv. Funct. Mater.* **2005**, *15*, 1683.
(12) Jo, B.-H.; van Lerberghe, L. M.; Motsegood, K. M.; Beebe, D. J. *Microelectromech. Syst.* **2000**, *9*, 76.
(13) Wu, H.; Odom, T. W.; Chiu, D. T.; Whitesides, G. M. *J. Am. Chem. Soc.* **2003**, *125*, 554.
(14) DeBolt, L. C.; Mark, J. E. *Macromolecules* **1987**, *20*, 2369.
(15) Kim, E.; Xia, Y.; Zhao, X.; Whitesides, G. M. *Adv. Mater.* **1997**, *9*, 651.
(16) Lee, J. N.; Park, C.; Whitesides, G. M. *Anal. Chem.* **2003**, *75*, 6544.
(17) Campbell, M.; Sharp, D. N.; Harrison, M. T.; Denning, R. G.; Turberfield, A. J. *Nature*, **2000**, *404*, 53.
(18) Ullal, C. K.; Maldovan, M.; Chen, G.; Han, Y.; Yang, S.; Thomas, E. L. *Appl. Phys. Lett.* **2004**, *84*, 5434.
(19) Feng, R.; Farris, R. J. *J. Micromech. Microeng.* **2003**, *13*, 80.
(20) Hong, G.; Holmes, A. S.; Heaton, M. E. *Microsyst. Technol.* **2004**, *10*, 357.
(21) Chatzichristidi, M.; Raptis, I.; Argitis, P.; Everett, J. *J. Vac. Sci. Technol., B* **2002**, *20*, 6, 2968.
(22) Moon, J.-H.; Yang, S. *J. Macromol. Sci., Part C* **2005**, *45*, 351.
(23) Deforest, W. *Photoresist*: *Materials and Processes*; McGraw-Hill Book Co., Inc.: New York, 1975; p 132.
(24) *Introduction to Microlithography*; Thompson, L. F., Willson, C. G., Bowden, M. J., Eds.; ACS Symposium Series, No. 219; American Chemical Society: Washington, DC, 1994; p 139.
(25) Gorishnyy, T.; Ullal, C. K.; Maldovan, M.; Fytas, G.; Thomas, E. L. *Phys. Rev. Lett.* **2005**, *94*, 115501.
(26) Goldfarb, D. L.; de Pablo, J. J.; Nealey, P. F.; Simons, J. P.; Moreau, W. M.; Angelopoulos, M. *J. Vac. Sci. Technol., B* **2000**, *18*, 3313.
(27) Raccurt, O.; Tardif, F.; Arnaud d'Avitaya, F.; Vareine, T. *J. Micromech. Microeng.* **2004**, *14*, 1083.
(28) Yang, S.; Megens, M.; Aizenberg, J.; Wiltzius, P. Chaikin, M. C.; Russel, W. B. *Chem. Mater.* **2002**, *14*, 2831.

NL052577Q